World Conference on Timber Engineering Oslo 2023

Seismic Performance Evaluation of a Traditional Wooden Townhouse that did not Collapse in the 2016 Kumamoto Earthquake

Yasuhiro Nambu[1], Toshihiko Ninakawa[2], Hiroki Tabata[3] and Akio Kitahara[4]

ABSTRACT: This study presented the results of the structural investigation of a *machiya*, a traditional Japanese wooden townhouse, located in Kumamoto City, which is not significantly damaged during the 2016 Kumamoto earthquake. The seismic performance of the house was evaluated using the limit strength calculations. In addition, the effect of through columns, which were present various parts of the house, was considered using a simplified model. Time history response analyses were conducted using the observed ground motion records, and the differences in the maximum response story drift due to the presence or absence of through columns were investigated. The following findings were obtained. 1) The main house had no full mud walls in the ridge direction on the first story, and most of the columns were through columns. 2) The base shear coefficients for the main house were 0.02 in the ridge direction for a story drift of 1/60 rad. The horizontal resistance was considerably small. However, the house did not collapse during the 2016 Kumamoto earthquake. 3) Time history response analyses were conducted with and without considering through columns, and the results showed that the maximum response story drift in the first story was reduced by 10-45% when the effect of through columns was considered.

KEYWORDS: Traditional wooden building, Japanese townhouse, time history response analysis

1 INTRODUCTION

In 2016, a series of earthquakes struck Kumamoto, a prefecture in Japan's southern island of Kyushu. The first earthquake, with a magnitude of 6.2, occurred on April 14th, followed by a second earthquake, with a magnitude of 7.0, on April 16th. These earthquakes caused widespread damage and loss of lives in the region. Many traditional wooden townhouses called *machiya* in Furumachi, Kumamoto-shi were also damaged by earthquakes (the PGA of the nearest earthquake observation record was 432 gal for the foreshock and 552 gal for the mainshock [1]), and several *machiyas* confirmed to have collapsed [2, 3]. However, not all *machiyas* that do not meet current Japanese seismic regulations suffered serious damage. To gain new insights into improving the seismic performance evaluation method of *machiyas*, we focused on several *machiyas* that were not severely damaged by the earthquakes and still exist in the town. Therefore, we investigated one existing *machiya* in Furumachi to understand the structure and evaluated its seismic performance at the time of the earthquakes. This paper reports the results of the structural investigation and the evaluation of seismic performance through time history response analysis.

2 TARGET HOUSE AND DAMAGE SITUATION

Figure 1 shows the exterior and interior of the target house. The target house was built around 1915–1917.

(a) South (front) exterior

(b) Interior (2nd story, facing north)

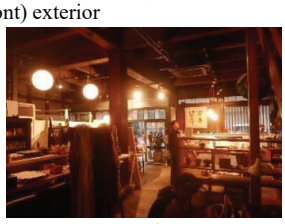

(c) Interior (1st story, facing south)

***Figure 1**: Exterior and interior views (taken on 10/18/2019)*

[1] Yasuhiro Nambu, Dr. Eng., Assist. Prof., Kyushu University, Japan, nambu@arch.kyushu-u.ac.jp
[2] Toshihiko Ninakawa, Dr. Eng., Prof., Kyushu University, Japan, ninakawa@arch.kyushu-u.ac.jp
[3] Hiroki Tabata, M. Eng, Kyushu University (present affiliation is Ministry of Land, Infrastructure, Transport and Tourism), Japan, tabata-h8310@mlit.go.jp
[4] Akio Kitahara, Dr. Eng., Prof., Pref. Univ. Kumamoto, Japan, kitahara@pu-kumamoto.ac.jp

https://doi.org/10.52202/069179-0535

The building was originally a store that handled oil and wheat; thus, brick walls were built on the gable side of the site boundary from the beginning to prevent fire. In 1992 and 2007, renovation work was carried out on the main building, and reinforcing steels were attached to the brick wall on the west side at that time. Then, the damage situation during the 2016 Kumamoto earthquake is described.

Figure 2 shows the damage situation of the main house of the residence (taken on May 14, 2016).

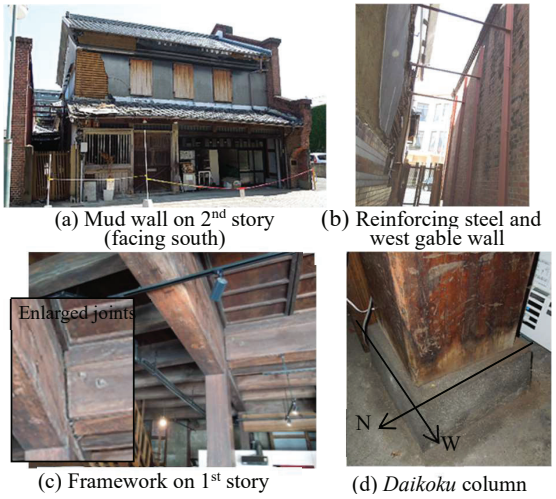

(a) Mud wall on 2nd story (facing south) (b) Reinforcing steel and west gable wall

(c) Framework on 1st story (d) *Daikoku* column

***Figure 2**: Damage after the earthquake (Photo taken 5/14/2016)*

As shown in Figure 2(a), the mud wall on the west side collapsed on the south (front) and north (back) sides of the 2nd story of the house. On the west gable end, as shown in Figure 2(b), the mud wall around the column where the reinforcing steels of the brick wall are connected collapsed. Inside the house, there was some deformation at some of the joints in the framing where wooden pegs were used, and there was some looseness, such as the horizontal timber coming out of the column, as shown in Figure 2(c), but no major damage, such as a broken column, was confirmed. As shown in Figure 2(d), the base of the pillar of the *daikoku* column located near the center of the house had rotated slightly clockwise, based on the marks remaining on the foundation stone, and had moved about 1 cm to the east as a whole. As there was no major damage, the house was repaired by repainting the mud wall and is still in use today [3].

3 STRUCTURAL INVESTIGATION

We conducted a field survey of the house on November 18, 2019. We measured each part of the house as part of a structural investigation, created floor plans and elevation drawings, and identified the structural elements and types of the house. In addition, we conducted microtremor measurements as a vibration survey, but the results are not reported in this paper (refer to [4 for the results]).

The structure of each part is shown in Figure 3, and the framework and floor plan of the house are shown in Figures 4 and 5, respectively.

(a) Cross beam (b) Diagonal strut

***Figure 3**: Structure of each part (taken on the day of the structural investigation)*

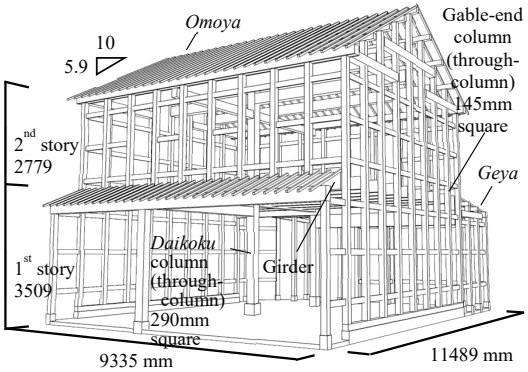

***Figure 4**: Framework of target house (from the south)*

The house consists of a two-story main house called *Omoya* and attached east and west side structures called *Geya*. The height of each story is 3,509 mm (from the ground to the top of the beam) for the first story and 2,799 mm (from the top of the second-floor beam to the top of the purlins) for the second story. The column bases are placed on the top of the foundation stones and not anchored to them. All the gable-end columns are 145 mm square cross-section, and the *daikoku* column (central supporting pillar) is 290 mm square cross-section.

The gable-end columns are spaced at 910-mm intervals and are through columns that reached the purlins, with ridge beams and purlins tenoned into them to form through-column structures. Here, the "cross beams" in Figure 5 represent the beams mortised into the columns. The species of the framework could not be identified. The gable-end exterior walls of the *Omoya* are entirely mud walls, while the non-gable sides have no exterior walls on the first story and are mainly mud walls on the second story. The wall thickness of the exterior walls is approximately 130 mm on both the gable-end and non-gable sides. Additionally, the visible penetrating tenons (called *nukis*) are in the interior side of the exterior walls. The cross-sectional dimensions of the *nuki* includes a width of 30 mm and a depth of 145 mm, with three levels installed on each story's mud walls. There are no interior walls. The first floor is a dirt floor, and the second floor is a board floor. At the level of the roof beam level, diagonal struts measuring 120-mm width and 160-mm depth were installed. The roof is covered in pantile roof for both the *Omoya* and *Geya*. The east-west brick walls are laid in English bond with a thickness of 460 mm. The west brick wall is reinforced with equal-angle steel sections with a width of 100 mm and height of 100 mm (thickness unmeasured) and is connected to the gable-end columns of the *Omoya*, with three reinforcements installed at 910-

https://doi.org/10.52202/069179-0535

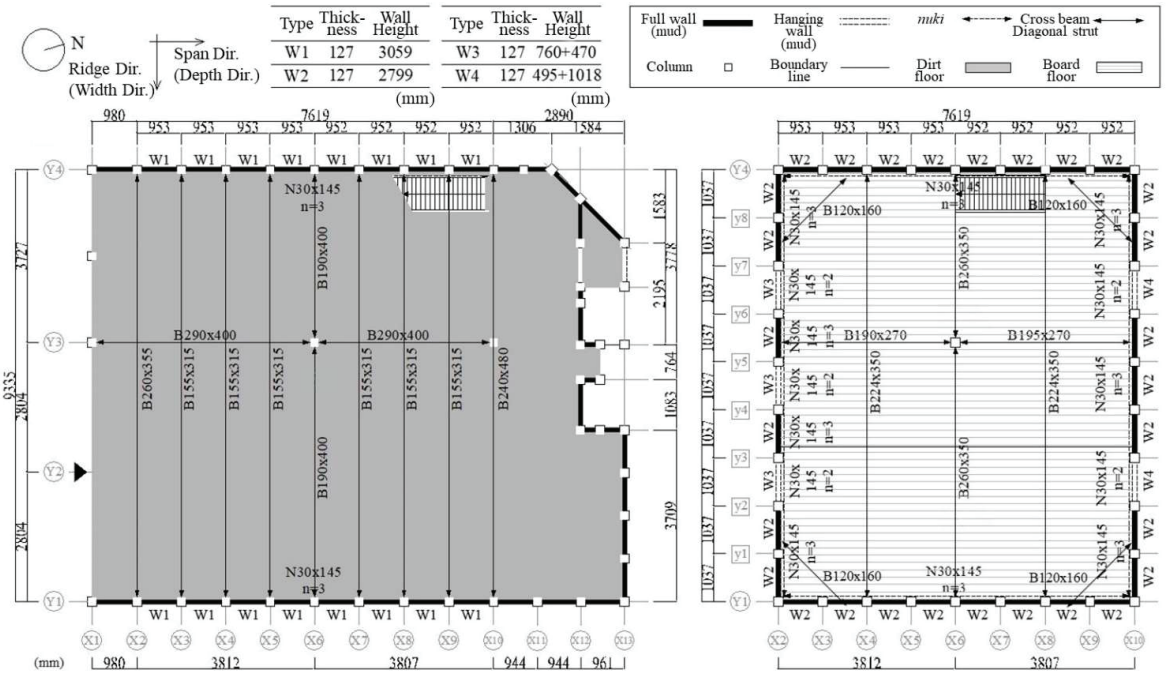

(a) 1st story (Only dirt floor show ground level) (b) 2nd story (Only board floor show 2nd floor level)

***Figure 5**: Floor Plan (mm)*

mm intervals. The east brick wall and the gable-end of the *Omoya* are in contact, but the details of the contact area are not visible. It should be noted that there is a wooden detached house on the north side of the property, separated by a courtyard, but it is not structurally connected to the *Omoya*.

4 SEISMIC PERFORMANCE EVALUATION BY LIMIT STRENGTH CALCULATION

The seismic performance of the target house was evaluated using the limit strength calculation, which is generally used to evaluate the seismic performance of traditional wooden buildings. The calculations were based on [6]. The skeletal curves of the house were calculated from the bearing elements, such as the full mud walls, hanging walls, and column-beam joints, and the response values during earthquakes were obtained using the response spectrum method with equivalent linearization. This report gives an overview of the influence of through columns as a starting point for evaluating the seismic performance of the target house. Therefore, the influence of the *Geya* and brick walls were ignored to simplify the analysis.

4.1 CALCULATION OF WEIGHT

The weight of the first story was calculated as the weight from the upper half of the first story to the lower half of the second story, and the weight of the second story was calculated as the weight from the upper half of the second story to the roof. The weight was calculated by multiplying the area of each part of the house by the fixed and live loads specified in Articles 84 and 85 of Order for Enforcement of the Building Standards Act of Japan, respectively, and the values in [5]. The live load is 600 N/m^2 in residential rooms when calculating seismic forces. The thickness of the mud wall is assumed to be 127 mm (obtained by subtracting the distance of 18 mm between the column surface and the wall surface from the column section dimension of 145 mm), and the roof is assumed to be covered with clay pantiles. The weight of the structural frame was calculated by multiplying the volume of each member by the specific gravity provided in [5] and assuming cedar for the columns and Oregon pine for the beams. Table 1 presents the calculated values of weight and mass, along with the floor area and height of each story.

***Table 1**: Results of weight and mass calculation*

	Weight [kN]	Mass [kg]	Floor area [m^2]	Story height [m]	Weight per unit area [kN/m^2]
2nd story	236.9	24150	71.1	2.799	3.33
1st story	183.8	18740	71.1	3.509	2.58
Total	420.7	42890	142.2	6.308	2.96

4.2 SKELETON CURVES

The skeleton curve of the target house was obtained by summing the skeleton curves of the bearing elements for each story and direction. The bearing elements considered include the full mud wall, hanging wall, *nukis*, and column-beam joints. The skeleton curves for each bearing element were determined based on [6]. It is assumed that all mud walls fail in shear. The skeleton curve of the column-beam joints was obtained by assuming that the bending moment M at the joint (using the dowel-and-

mortise joint "*one-hozo komisen-uchi*") is equally distributed between the upper and lower floor columns. Then, the resulting M was divided by the height of each story to obtain the shear force Q and R curves. The M and θ curves used here for the dowel-and-mortise joint were determined based on [6], and it was assumed that θ was equal to the story drift angle R. The results of the skeleton curve calculation are shown in Figure 3.

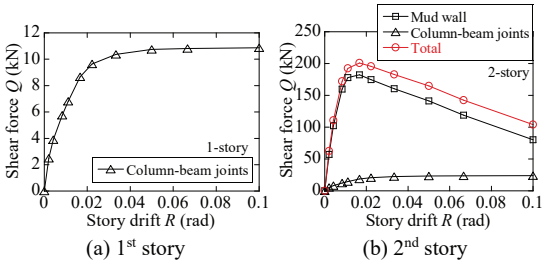

***Figure 6**: Skeleton curves for each story*

In the ridge direction, the lateral resistance of the first story is extremely small compared to that of the second story. It should be noted that the base shear coefficient C_y, which is obtained by dividing the shear force at the first story drift of 1/60 rad by the total weight of the *Omoya*, is 0.40 in the span direction and 0.02 in the ridge direction, indicating that the value in the ridge direction is extremely small.

4.3 MAXIMUM RESPONSE STORY DRIFT

The limit strength calculations were performed using the weight and skeleton curve data. The input data is based on the Japanese design response spectrum, which assumes Type 2 ground classification. The damage limit for rare earthquakes was evaluated using a story drift angle of 1/120 rad, while the safety limit for very rare earthquakes was evaluated using a story drift angle of 1/20 rad [6]. The maximum response story drift angle in each direction is listed in Table 2. Here, "rare earthquakes" and "very rare earthquakes" are input seismic motions used in the structural design in Japan. These earthquakes are classified based on their rarity and represent the maximum seismic force that a building may experience during its lifetime. Specifically, "rare earthquakes" refer to earthquakes that are expected to occur once in approximately 50 years, while "very rare earthquakes" refer to those that are expected to occur once in 500 years.

***Table 2**: Results of weight and mass calculation*

	Target response spectrum	Limit [rad]	Max. response story drift [rad]	
			1st story	2nd story
Span direction	Rare	1/120	1/309	1/518
	Very rare	1/20	1/24	1/242
Ridge direction	Rare	1/120	1/47	1/2731
	Very rare	1/20	No response	

The maximum response story drift in the span direction is within the damage and safety limits for each story. However, the maximum response story drift in the ridge direction is significantly larger on the first story compared to the span direction, and the response value cannot be obtained in the event of a very rare earthquake, resulting in significant seismic performance deficiencies.

As a result, the target house did not collapse during the Kumamoto earthquake even though, based on the limit strength calculations, it would experience a significantly large maximum response story drift in the ridge direction when subjected to seismic motion equivalent to a very rare earthquake. The target house has relatively large through columns, which are not considered in the limit strength calculations. It is speculated that these through columns may affect the seismic performance because the horizontal resistance in the ridge direction at the first story is extremely low. In the following section, we investigate this possibility using time history response analysis.

5 SEISMIC PERFORMANCE EVALUATION BY TIME HISTORY RESPONSE ANALYSIS

In this section, time history response analysis is conducted using a model that considers through columns and a model that does not consider them in the ridge direction of the target house, and the seismic performance of the house is evaluated based on the results.

5.1 ANALYSIS METHOD

We assumed the house to have no torsional motion on a rigid floor and modeled it as a two-mass system. An overview of the analysis model is shown in Figure 7. For the ridge direction, two types of models were used: a model without through columns (referred to as the NTC model; see Figure 7(a)) and a model with through columns (referred to as the TC model; see Figure 7(b)). The through columns were assumed to be linear elastic bodies and modeled with pinned connections to each mass point via rigid beams. Note that the connections between the through columns and the ground were assumed to be pinned.

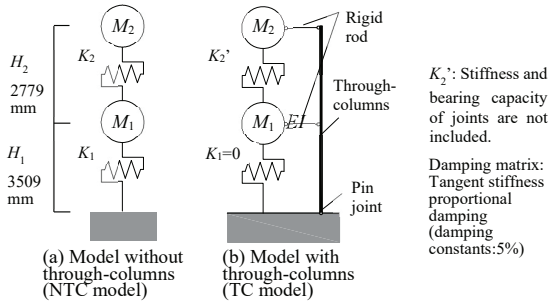

***Figure 7**: Overview of analysis models*

The restoring force characteristics (skeleton curve + history characteristics) of the equivalent shear springs K_1 and K_2 on each story are determined by the bi-linear + slip model, which is the sum of the bi-linear and tri-linear slip

https://doi.org/10.52202/069179-0535

models, representing the history characteristics of the wooden structure (Figure 8).

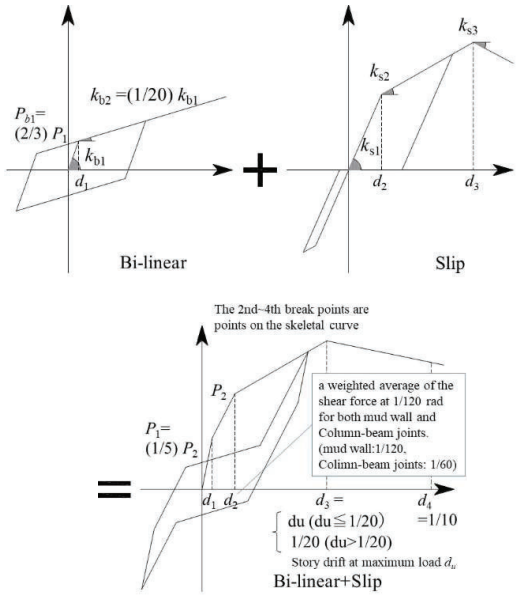

***Figure 8**: Hysteresis model*

The equivalent shear springs K_1, K_2, and K_2' on each model's story are determined as follows: K_1 and K_2 are based on the skeleton curve calculated in the previous section, while K_2' is based on the skeleton curve obtained by subtracting the skeleton curves of the column-beam joints from the skeleton curve of K_2.

The skeleton curves of the equivalent shear springs K_1, K_2, and K_2' for each model are determined as follows:

1) The second breaking point (yield point) was determined as a point on the skeleton curve of each story of the target house, and the story drift at the breaking point was determined based on the inter-story shear force ratio of the mud walls and column-beam joints. Specifically, the story drift of the second breaking point was assumed to be 1/120 rad when only the mud wall was present, and it was assumed to be 1/60 rad when only the column-beam joint was present. When both elements were present, the inter-story shear force at 1/120 rad of both elements was used as a weight to determine the story drift of the second breaking point by weighted averaging.

2) The third breaking point (ultimate point) was taken as a point on the skeleton curve of each story of the target house and set to the value of the story drift R_u at the maximum load. However, if R_u > 1/20, it was taken as the point at 1/20 rad.

3) The degraded stiffness was set to the stiffness connecting the third breaking point and the point on the skeleton curve of the target house at a story drift of 1/10 rad.

The validity of the above settings must be verified in future studies. Figure 9 shows the skeleton curves of the shear springs on each story used in this study, together with the skeleton curves calculated in the previous section. The analysis limit was the intersection of the degraded stiffness of the slip model and the horizontal axis (inter-story shear force = 0), and the analysis was terminated at the point of intersection.

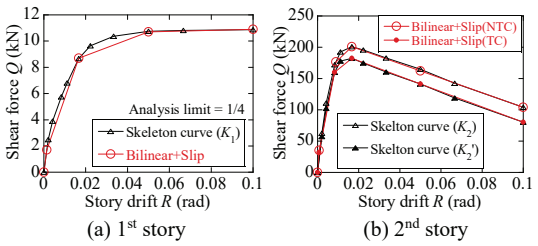

***Figure 9**: Skeleton curves of shear springs for each story*

The history characteristics were assumed to be the same as in [7]. The relationship between the first breaking point load P_1 and the second breaking point load P_2 for the bi-linear + slip skeleton curve is expressed by the following equation [7]:

$$P_1/P_2 = 1/5. \quad (1)$$

The ratio of the bi-linear component at the first breaking point P_{b1}/P_1 is given by the following equation [7]:

$$P_{b1}/P_1 = 2/3. \quad (2)$$

The ratio of the second to first bi-linear component stiffness k_{b2}/k_{b1} is assumed as the following [7]:

$$k_{b2}/k_{b1} = 1/20. \quad (3)$$

The through columns exert horizontal resistance when there is a difference in the story drift between the first and second stories. The relationship between the external force and the deformation acting on through columns is shown in Figure 10 [8].

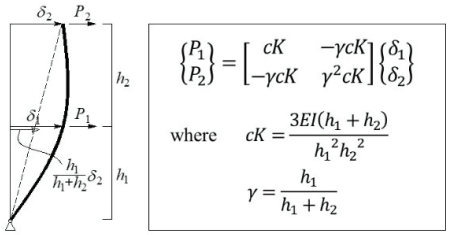

***Figure 10**: Through columns modeling* [8]

Through columns are assumed to be linear elastic. The stiffness matrix of the TC model was obtained by adding the stiffness matrix of the through columns shown in the figure to that of the NTC model. The second moment of area I for the through columns was calculated by adding the second moment of area I_c and I_{cd} for each of the 18 gable-end columns with a cross-section of 145 mm and the central column (*Daikoku* column) with a cross-section of 290 mm. The columns were assumed to be made of

cedar, and the elastic modulus E was used as the basic elastic modulus for an ungraded lumber, $E_0 = 7.0$ kN/mm^2, from [9].

In addition, for the through columns, the failure due to bending moments M_c and M_{cd} at the first-floor column head of each of the gable-end and *daikokubashira* columns, respectively, is considered based on the difference in story drifts between the first and second stories. M_c and M_{cd} were calculated using the following equations based on the maximum difference in story drifts $|R_2 - R_1|_{max}$ obtained from the time history response analysis:

$$M_c = \frac{3EI_c}{H_1 + H_2}|R_2 - R_1|_{max} + M_\theta, \quad (4)$$

$$M_{cd} = \frac{3EI_{cd}}{H_1 + H_2}|R_2 - R_1|_{max} + 2M_\theta, \quad (5)$$

where M_θ is taken as the maximum bending moment at the column-beam joint (M_θ = 4.0 kNm). H_1 and H_2 indicate the height of each story, respectively.

An additional $2M_\theta$ is added for the *Daikoku* column as two beams are attached in the ridge direction. However, when considering through column failure, it does not consider the maximum bending moment at the column-beam joints M_θ in the TC model. The bending strength of each column $M_{cu}$and M_{cdu} was calculated by multiplying the reference strength F_b of the column by the effective section modulus Z_e, where Z_e is 3/4 of the full section modulus Z of the column considering the section deficiency (M_{cu} = 8.5 kNm and M_{cdu} = 67.7 kNm). The bending strength F_b of the column was taken as the average value of H1, E70 (cedar) in [10], which was 40.9 kN/mm^2. If the bending moment M_c or M_{cd} generated in each column exceeds the bending strength (M_{cu} or M_{cdu}), the column was considered to have failed.

The mass matrix was calculated using the masses of each story, M_1 and M_2, as determined in the previous chapter. The story heights, H_1 and H_2, were determined based on the results of the structural investigation presented in Section 3. The damping was assumed to be proportional to the instantaneous stiffness, and the damping coefficient was set to 5%. The P-Δ effect was not considered in this study.

Figures 11 and 12 show observation points of the input seismic waves and the seismic waveforms and acceleration response spectra, respectively.

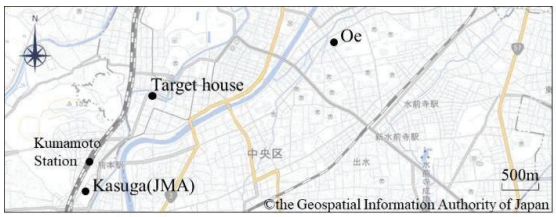

***Figure 11**: Target house and earthquake observation sites*

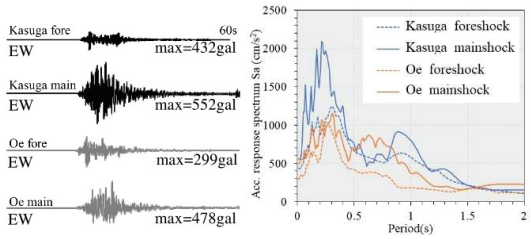

(a) Input earthquake (b) Response Spectrum

***Figure 12**: Target house and earthquake observation sites*

The input seismic waves were based on the observed seismic waves of the 2016 Kumamoto earthquake [11], using the fore and main shock observed seismic waves at the observation points near the target house in Kasuga, Nishi-ku, Kumamoto City and Oe, Chuo-ku, Kumamoto City. The seismic waves used were the EW component corresponding to the ridge direction of the target house. In addition to the input of the mainshock, continuous earthquake ground motions with an interval of 60 s between the fore and main shock were also considered in this study.

5.2 ANALYSIS RESULTS AND EFFECT OF THROUGH COLUMNS

In this study, the relationship between the inter-story shear force and the story drift for each floor obtained from the analysis is shown in Figure 13 using the example of continuous input of observed earthquake waves in Oe. The results of the NTC model are shown in (a) and (b) while those of the TC model are shown in (c) and (d). Furthermore, the time history changes of the story drift for the first story are shown in Figure 14.

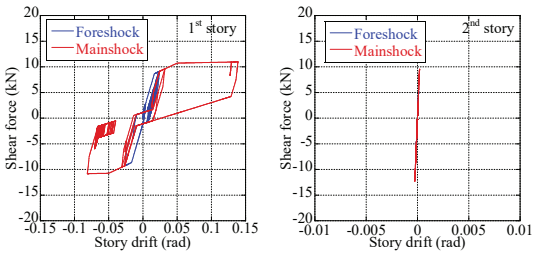

(a) NTC model

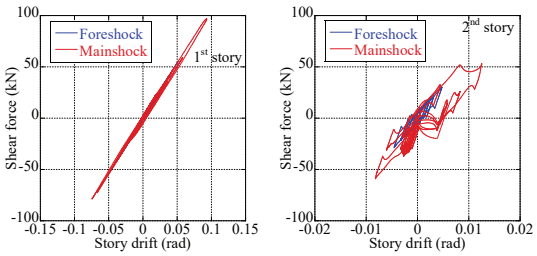

(b) TC model

***Figure 13**: Relationship between the inter-story shear force and the story drift (input: Oe continuity)*

https://doi.org/10.52202/069179-0535

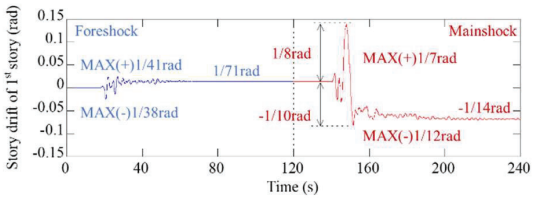

(a) NTC model

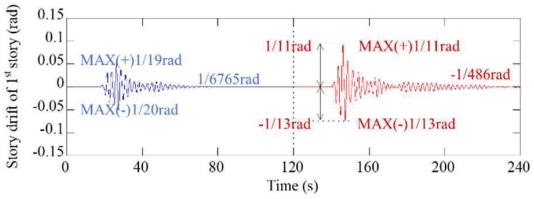

(b) TC model

***Figure 14**: Time history changes of story drift for the first story (input: Oe continuity)*

In the TC model, the second story deforms elastically within its range, while only the first story undergoes significant deformation. In comparison to the NTC model, the maximum response story drift of the first story in the TC model decreases by approximately 36% from 1/7 rad to 1/11 rad. Furthermore, for the second story, the ratio of the maximum response story drift to that of the first story is approximately 0.2% in the NTC model, but it increases to approximately 14% in the TC model, and the second story undergoes plastic deformation in the TC model. These results confirm the effectiveness of through columns in equalizing the story drifts of each story. It is apparent that residual deformation from the foreshock remains in the NTC model based on the observation of the time history response of the story drift of the first story, while it is not observed in the TC model. These tendencies were also observed with the Kasuga seismic input.

Table 3 summarizes the results of time history response analysis for four input ground motions, each analyzed in eight patterns with and without through columns considered. M_c/M_{cu} and M_{cd}/M_{cdu} represent the ratios of the bending moment to the bending strength of the gable-end columns and the Daikoku column, respectively. The ratio of 1.0 or greater indicates that the column is prone to breaking.

***Table 3**: Analysis results*

Earthquake		Model	Max. response story drift (rad)		Residual story drift of 1st story (rad)	Max. bending moment of column (kNm)		M_c/M_{cu}	M_{cd}/M_{cdu}
			1st story	2nd story		M_c	M_{cd}		
Kasuga	main shock	NTC	1/15	1/4122	1/20	12.0	135.5	0.8	1.1
		TC	1/17	1/178	1/4216	6.5	104.3	0.4	0.8
	continuity	NTC	1/9	1/4595	1/44	17.3	220.5	1.1	1.8
		TC	1/17	1/181	1/4900	6.5	104.4	0.4	0.8
Oe	main shock	NTC	1/9	1/3644	1/22	17.9	230.7	1.1	1.9
		TC	1/11	1/79	1/531	10.0	159.6	0.6	1.3
	continuity	NTC	1/7	1/3819	1/14	21.0	280.2	1.3	2.2
		TC	1/11	1/80	1/486	10.0	159.7	0.6	1.3

The results of the time history response analysis for the NTC model show that the maximum response story drift of the first story exceeded the safety limit of 1/20 rad, reaching 1/15 and 1/9 rad for the Kasuga and Oe mainshocks, respectively (Table 3). However, the limit strength calculations indicate that the NTC model collapses in a very rare earthquake, as shown in Table 2. Although the earthquake characteristics and intensities assumed in the time history response analysis and the limit strength calculations are different, the results of both methods are not significantly contradictory.

Figure 15 shows the maximum response story drift of the first story for each model and input.

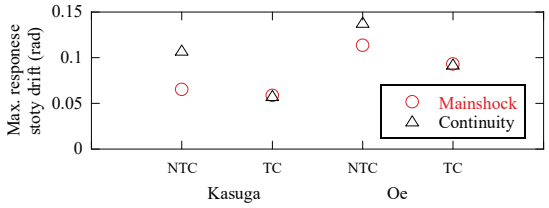

***Figure 15**: Absolute value of the maximum response story drift for the 1st story*

The response story drift of the first story is larger for the continuous input than for the mainshock input. In the TC model, the maximum response story drift of the first story was reduced by approximately 10–20% for the mainshock input and 33–45% for the continuous input compared to the NTC model. Additionally, in the TC model, no residual deformation was observed in the foreshock due to the seismic input used in this study, resulting in similar response values for the continuous input and mainshock input alone. Although the maximum response story drift of the first story exceeded the safety limit of 1/20 rad established in Section 4.3 for both models, the analytical results suggest that the through columns act as bearing elements and suppress the story drift of the first story.

In the target house, according to Table 3, the result of the Kasuga and Oe mainshocks was the breaking of the gable-end column or the Daikoku column in the NTC model, while only the Daikoku column broke due to continuous input from the Oe mainshock in the TC model. It should be noted that there were no through column breakage that was confirmed as damage in the 2016 Kumamoto earthquake for the target house.

Subsequently, the residual story drift for each model and each seismic input for first story is shown in Table 3 and Figure 16.

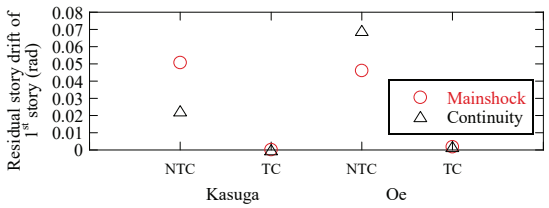

***Figure 16**: Absolute value of the residual story drift for 1st story*

https://doi.org/10.52202/069179-0535

For all cases, the residual story drift for each model was smaller in the TC model than in the NT model, suggesting that the through-column had the effect of reducing the residual story drift. However, in this study, it should be noted that for the TC model, there was no plasticization observed for the second story to generate residual story drift during the foreshock. Moreover, the assumption was made that the through column was a linear elastic body, and that the through column and each mass point were connected by rigid bars (rigid floor assumption), which may have increased the effect of the through column.

6 CONCLUSIONS

This study presented the results of the structural investigation of a machiya, a traditional Japanese wooden townhouse, located in the historic district of Furumachi in Kumamoto City, which is not significantly damaged during the 2016 Kumamoto earthquake. The seismic performance of the house was evaluated using the limit strength calculations commonly used for assessing the seismic performance of traditional wooden townhouses. In addition, the effect of through columns, which were present various parts of the house, was considered using a simplified model. Time history response analyses were conducted using the observed ground motion records from the earthquakes that occurred in Kasuga and Oe in 2016, and the differences in the maximum response story drift due to the presence or absence of through columns were investigated. The following findings were obtained.

1. The main house (Omoya) had no full mud walls in the ridge direction on the first story, and the gable-end columns (145 mm square cross-section) and a Daikoku column (290 mm square cross-section) were reached to the purlins, forming a post-dominant structure.
2. The base shear coefficients for the main house were 0.4 in the span direction and 0.02 in the ridge direction for a story drift of 1/60 rad. The horizontal resistance in the ridge direction was considerably small. If the effect of through columns is not considered in the limit strength calculation, the maximum response story drift in the first story in the ridge direction would be extremely large, but the house did not collapse during the 2016 Kumamoto earthquake.
3. Time history response analyses were conducted with and without considering through columns, and the results showed that the maximum response story drift in the first story was reduced by 10–20% during the mainshock and by 33–45% during continuous input when the effect of through columns was considered.

Therefore, it is suggested that through columns act as bearing elements, potentially reducing the maximum response story drift in the first story. However, it should be noted that the results are subject to assumptions, such as the validity of the rigid floor assumption and the linear elastic behavior of through columns. Furthermore, the stiffness of the second story was much larger than that of the first story. Based on these results, we developed a method for incorporating the effect of through columns into the limit strength calculations.

ACKNOWLEDGEMENT

We would like to express our sincere gratitude to the owners and stakeholders of the target house, Mr. Michikiyo Yamakawa of Kumamoto Association of Architects & Building Engineers, and the students of the Kitahara Laboratory at Prefectural University of Kumamoto and the Ninakawa Laboratory at Kyushu University for their invaluable support in conducting the structural investigation. Without their generous cooperation, this study would not have been possible.

REFERENCES

[1] Japan Meteorological Agency: Seismic Intensity Map, https://www.data.jma.go.jp/

[2] Kurashige K., Kitahara A. and Miyazato A.: Earthquake Damage of Wooden Buildings in the Kumamoto City due to the 2016 Kumamoto Earthquake, AIJ Kyushu Chapter architectural research meeting, No.56, pp605-608, 2017.3. (in Japanese)

[3] Architectural Institute of Japan: Report on the Damage Investigation of the 2016 Kumamoto Earthquakes, pp112-113, 2018.6. (in Japanese)

[4] Nambu Y., Tabata H., Kitahara A. and Ninakawa T.: Structural Performance Evaluation of Townhouses that did not Collapse in the 2016 Kumamoto Earthquake - A Townhouse with Continuous Columns in Furumachi, Kumamoto City - Part2: Microtremor Measurement Result and Limit Strength Calculation, Architectural Institute of Japan Summaries of technical papers of annual meeting, C-1, pp.633-634, 2020.9. (in Japanese)

[5] Architectural Institute of Japan: Recommendations for Loads on Buildings (2015), p132, 2015.2. (in Japanese)

[6] The editorial committee of design manual for traditional wooden buildings: A manual of aseismic design method for traditional wooden buildings including specific techniques for unfixing column bases to foundation stones, Gakugei Shuppansha, 2019.6. (in Japanese)

[7] Isoda H., Kawai N.: HYSTERESIS MODEL OF WALLS ON JAPANESE CONVENTIONAL CONSTRUCTION: Study on seismic behavior of wooden construction, Journal of Structural and Construction Engineering (Transactions of AIJ), Vol.72, No. 616, pp.157-163, 2007. 6. (in Japanese)

[8] Architectural Institute of Japan: Recommendation for Structural Calculation of Traditional Wood Buildings by Calculation of Response and Limit Strength, 2013.2. (in Japanese)

[9] Architectural Institute of Japan: Standard for structural design of timber structures, 2006.

[10] Forestry and Forest Products Research Institute (強度性能研究会 : Strength and Performance Research Group): 「製材品の強度性能に関するデータベース」データ集(Database on Strength and Performance of Lumber Products)

[11] Japan Meteorological Agency: Strong-motion observation data, https://www.data.jma.go.jp/

https://doi.org/10.52202/069179-0535